ISSN 1027-5495. Functional Materials, 27, No.2 (2020), p. 354-362.
doi:https://doi.org/10.15407/fm27.02.354

Influence of titanium diboride particles size on the structure of TiB_2–(Fe–Mo) composite materials

***O.P.Umanskyi*[1], *M.S.Storozhenko*[1], *O.E.Terentiev*[1], *V.B.Tarelnyk*[2], *V.P.Krasovskyy*[1], *V.E.Sheludko*[1], *I.S.Martsenyuk*[1], *O.D.Kostenko*[1]**

[1]J.Frantsevich Institute for Problems of Materials Science, National Academy of Sciences of Ukraine, 3 Krzhyzhanovsky Str., 03068 Kyiv, Ukraine
[2]Sumy National Agricultural University, 160 Kondratev Str., 40021 Sumy, Ukraine

Received October 10, 2019

The influence of titanium diboride particles size (9–10 μm, 2–3 μm, 500–700 nm) on the structure formation of TiB_2–80 wt.%(Fe–13 wt.%Mo) composite materials was investigated. The differential-thermal and electron-probe analyses have shown that a decrease in the size of TiB_2 particles up to 2–3 μm does not substantially influence on the composite materials structure formation. The structure of the investigated composite materials consists of an iron-based matrix, TiB_2 and Mo_2FeB_2 hard borides. The addition of nano-sized TiB_2 particles (70–100 nm) is unreasonable because this promotes dissolution and recrystallization processes of titanium diboride; as a result, their size increases up to 5–6 μm and large amounts of Fe–Fe_2B and Fe–Mo_2FeB_2 eutectics are formed.

Keywords: composite material, structure, titanium diboride, iron, molybdenum, eutectic.

Исследовано влияние размера частиц диборида титана (9–10 мкм, 2–3 мкм, 500–700 нм) на особенности формирования структуры композиционных материалов системы TiB_2–80 мас.%(Fe–13 мас.%Mo). Методом дифференциально-термического и микро-рентгеноспектрального анализов установлено, что уменьшение размеров частиц TiB_2 до 2–3 мкм не влияет существенно на формирование структуры композиционных материалов, которая состоит из матрицы на основе железа и твердых боридов TiB_2 и Mo_2FeB_2. Введение частиц TiB_2 размером 500–700 мкм нецелесообразно, так как приводит к интенсификации процессов растворения и перекристаллизации диборида титана, в результате чего их размер увеличивается до 5–6 мкм, а также к формированию эвтектической структуры Fe–Fe_2B и Fe–Mo_2FeB_2.

Дослідження впливу розміру частинок дибориду титану на структуру композиційних матеріалів системи TiB_2–(Fe–Mo). *О.П.Уманський, М.С.Стороженко, О.Є.Терентьєв, В.Б.Тарельник, В.П.Красовський, В.Є.Шелудько, І.С.Марценюк, О.Д.Костенко.*

Досліджено вплив розміру частинок дибориду титану (9–10 мкм, 2–3 мкм, 500–700 нм) на особливості формування структури композиційних матеріалів системи TiB_2–80 мас.%(Fe–13 мас.%Mo). Методом диференційно-термічного та мікро-рентгеноспектрального аналізів встановлено, що зменшення розмірів частинок TiB_2 до 2–3 мкм не впливає суттєво на формування структури композиційних матеріалів. Структура композиційних матеріалів системи складається з матриці на основі заліза та включень твердих боридів TiB_2 та Mo_2FeB_2. Введення частинок TiB_2 розміром 500–700 нм є недоцільним оскільки призводить до інтенсифікації процесів розчинення та перекристалізації дибориду титану, внаслідок чого їх розмір збільшується до 5–6 мкм, а також до формування великої кількості евтектик Fe–Fe_2B та Fe–Mo_2FeB_2.

1. Introduction

Scientific and technological progress requires the use of metal-ceramic materials in special applications under conditions of intensive wear at high loads and temperatures [1]. Refractory titanium compounds (TiC, TiB_2, TiN, TiCN, and $TiCrB_2$) attract a lot of attention to the development of wear-resistant composite materials due to their high hardness and melting point, low density [2–10]. In general, the operating properties of such composite materials are determined by the correct selection of ceramic and metallic components, their ratio, and size [11]. Good wetting between ceramics and metal alloy is the key factor in the production of composites with the desired properties. The ability to control the interaction of interfaces between the refractory and metal components is also important [11, 12].

The TiB_2–(Fe–Mo) composite material was developed for the protective coatings deposition at the Institute for Problems of Materials Science named after Frantsevich (Ukraine) [13]. In order to select the composition of the metallic phase, the wetting behavior of Fe–Mo alloys in contact with TiB_2 was investigated [14]. Additive 2–17 wt. % molybdenum into iron enhances the wetting process of titanium diboride. The TiB_2–(Fe–13 wt.% Mo) system is characterized by zero contact angles and some interaction leading to the formation of molybdenum-iron boride phases. Thus, brittle intermetallic phases do not form in this system [15]. That is why, the TiB_2–(Fe–13 wt.% Mo) composite powder materials were used for plasma coatings deposition. As shown in our previous study [16], the ratio between the refractory phase and metallic components significantly affects the structure and wear resistance of TiB_2–(Fe–13 wt.% Mo) plasma coatings.

It should be noted that the particle size of the refractory phase is also of great importance for providing necessary operating properties of the composite materials and coatings. In particular, with a decrease in the size of titanium diboride particles in the TiB_2–(Fe–Ni) composite material from 5 down to 2 μm, the relative density, hardness, bending strength, and toughness of cermets increase [17]. Therefore, a corresponding increase in the wear resistance of TiB_2–(Fe–13 wt.% Mo) coatings can be associated with a decrease in the size of titanium diboride particle.

Since the TiB_2–(Fe–13 wt.% Mo) system is characterized by a chemical interaction between the component of the refractory compound and the metallic alloy, the size of titanium diboride particle will affect the structure of the composite materials. With a decrease in the particle size of the refractory compound, the interface increases; thus, the chemical interaction will occur more intensively. So the aim of this work is to study the effect of the particle size of titanium diboride on the structural-phase composition of TiB_2–(Fe–13 wt.% Mo) composite materials.

2. Materials and methods

In order to determine the effect of the size of titanium diboride particle on the structure of TiB_2–(Fe–13 wt.% Mo composite materials, the specimens with different particle sizes of TiB_2, namely, 9–10 μm (specimen No. 1), 2–3 μm (specimen No. 2), and 70–100 nm (specimen No. 3), were prepared. For all the specimens, the ratio between the component of the refractory compound (TiB_2) and the metallic phase (Fe–Mo) was 1:4.

To prepare the TiB_2–80 wt.%(Fe–13 wt.% Mo) specimens, initial powders of titanium diboride (TU 6-09-03-7-75), iron (GOST 9879-74), and molybdenum (GOST 5909-79) produced at the Donetsk Plant of Chemical Reagents, were thoroughly mixed in appropriate ratios in an alcohol medium. The obtained mixture was briquetted under pressure in a steel die.

The compacted specimens of TiB_2–80 wt.%(Fe–13 wt.% Mo) composite materials were studied by differential thermal analysis (DTA) with a VDTA-8M unit. To perform the DTA, the specimens were placed in alumina crucibles and heated to 1570°C in argon medium. The heating rate was 40°C/min. Iron was used as a reference sample. From the DTA heating and cooling curves, temperature regions of heat effects were determined.

After the DTA measurements, the structure of the sintered specimens was studied with JEOL-9500FS and PEM-106 scanning electron microscopes.

The microhardness of individual phases was determined by the pressing with a Vickers diamond pyramid under a load of 0.1 N in a PMT-3 unit.

3. Results and discussion

Figure 1 shows DTA heating and cooling curves of the TiB_2–80 wt.%(Fe–13 wt.% Mo) composite materials with an initial particle size (d) of titanium diboride of 9–10 μm

(specimen No. 1), 2–3 μm (specimen No. 2), and 70–100 nm (specimen No. 3).

It should be noted that the DTA heating curves of the specimen No. 1 (TiB_2 particles of d = 9–10 μm) and the specimen No. 2 (TiB_2 particles of d = 2–3 μm) are very similar. Peaks on the DTA curves represent phase transformations during heating or cooling cycle. The DTA heating curves of both specimens show endothermic peaks between 1142°C to 1200°C and represent a phase transition from solid to liquid (melting). Moreover, an exothermic effect without temperature extreme is observed on the DTA heating curves in the temperature range of 1215–1550°C. On the DTA cooling curves of both specimens, 2 exothermic effects are noted. The first exothermic peak appears at 1160°C and gradually transforms into the second exothermic peak at 1122°C. The presence of two temperature peaks on the DTA cooling curve testifies the crystallization of two phases.

On the whole, the DTA heating and cooling curves of specimen No. 3 (TiB_2 with d = 70–100 nm) are similar to the DTA curves of specimens No. 2 and No. 3, but have some differences. In particular, the DTA heating curve of the specimen No. 3 has an endothermic peak at 1142°C, which gradually turns into an exothermic peak at 1175°C; that is 40°C lower compared to the DTA curves for No. 1 and No. 2 specimens. This indicates the intensification of the chemical interaction between the components of the TiB_2–80 wt.%(Fe–13 wt.% Mo) system with a decrease in the particle size of titanium diboride down to 70–100 nm. There are exothermic peaks on the DTA cooling curve of specimen No. 3, as well as on the DTA curves of No. 1 and No. 2 specimens; this indicates the crystallization of two phases.

Taking into account the DTA results, it is reasonable to conclude that a decrease in the particle size of titanium diboride down to 2–3 μm does not substantially affects the processes of chemical interaction in the TiB_2–80 wt.%(Fe–13 wt.% Mo) system. The intensification of chemical interaction occurs when the particle size of titanium diboride is less than 1 μm. To confirm the DTA results, the structure of TiB_2–80 wt.%(Fe–13 wt.% Mo) composites with different particle sizes of titanium diboride was studied.

The structure of specimen No. 1 (TiB_2 with d = 9–10 μm) consists of a gray metallic matrix where black grains and some inclusions of a white phase are distributed (Fig. 2). The metallic matrix is an iron-based solid solution (Fig. 2c, Table 1, spectrum 1). The molybdenum content in iron does not exceed 2 %, and the titanium content is no more than 1 %. Titanium diboride grains with a size of 6–8 μm are distributed in the matrix (Fig. 2c, Table 1, spectrum 2). The inclusions of the white phase with a size of 20–30 μm have a regular shape and their microhardness is 21–22 GPa. The microanalysis revealed that these inclusions contain 60 wt.% Mo, 24 wt.% Fe, 10 wt.% B, and 6 wt.% Ti (Fig. 2c, Table 1, spectrum 3); this makes it possible to identify this phase as Mo_2FeB_2 boride doped with titanium. It should be noted that in some areas (where titanium diboride grains are absent), the Fe–Fe_2B eutectic structure forms (Fig. 2d, Table 1, spectrums 4 and 5).

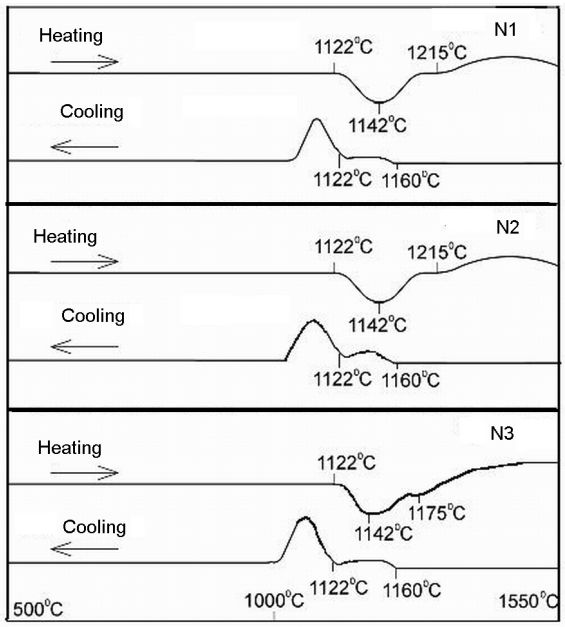

Fig. 1. DTA curves of TiB_2–80 wt.%(Fe–13 wt.% Mo) composite materials.

The structure of specimen No. 2 (TiB_2 with d = 2–3 μm) consists of inclusions of black and white phases distributed in the gray metallic matrix (Fig. 3). The matrix is an iron-based solid solution containing up to 2 wt.% molybdenum and up to 1 wt.% titanium (Fig. 3c, Table 2, spectrum 1). The microanalysis results show that black grains are titanium diboride particles with a size of 2–3 μm; this corresponds to their initial size (Fig. 3c, Table 2, spectrum 2). The white colored grains are composed of 24 wt.% Fe, 58 wt.% Mo, 10 wt.% B and

Table 1. Chemical composition of phases in the TiB_2–80 wt.%(Fe–13 wt.% Mo) composite material with the TiB_2 particle size of 9–10 μm

Figure	Spectrum	Element composition, wt.%				Phase
		Ti	Fe	Mo	B	
2c	1	1	98	1	0	Fe-based solid solution
	2	65	1	–	34	TiB_2
	3	6	24	60	10	Mo_2FeB_2
2d	4	0	99	1	0	Fe–Fe_2B eutectic
	5	1	89	2	8	

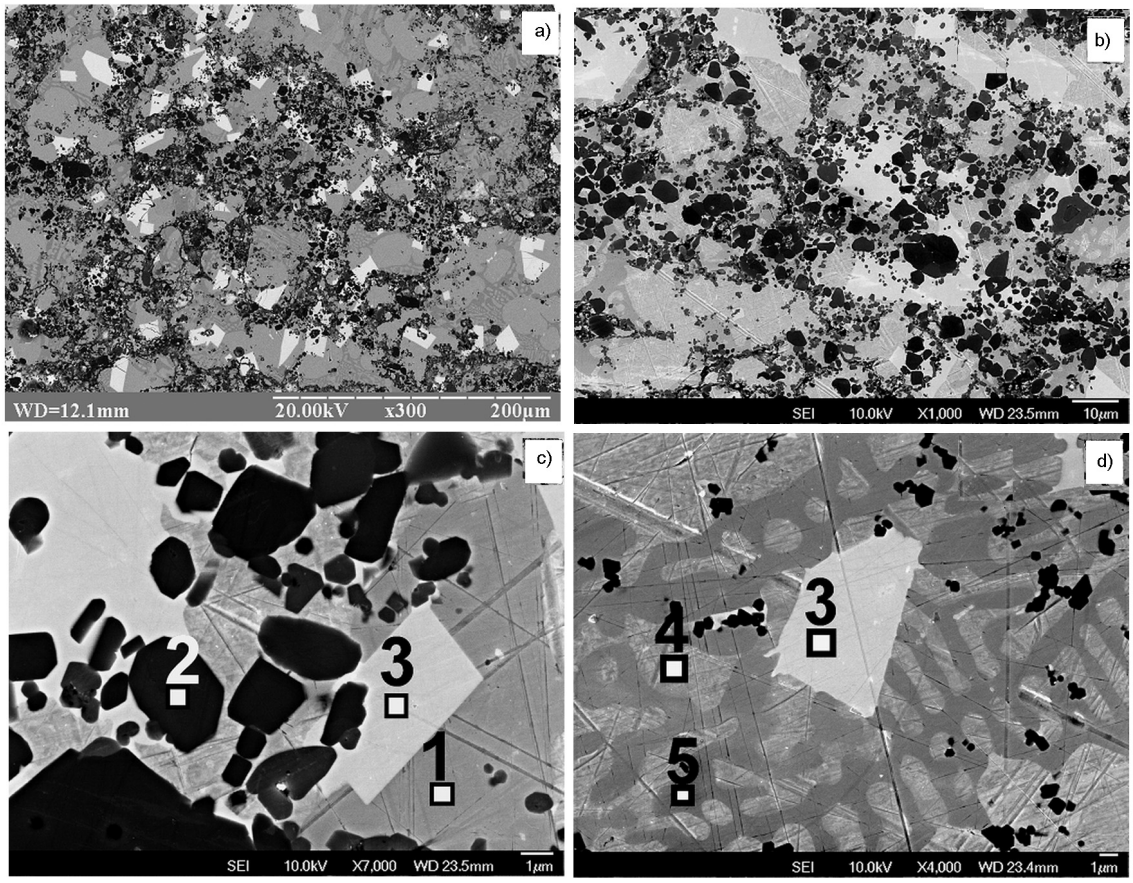

Fig. 2. Structure of the TiB_2–80 wt.%(Fe–13 wt.% Mo) composite material with TiB_2 particle size of 9–10 μm: (a, b) general view; (c) zone of borides formation; (d) zone of eutectic formation.

8 wt.% Ti (Fig. 3c, Table 2, spectrum 3). Their microhardness is 21–22 GPa and the size reaches 40–60 μm. Thus, the white grains are identical to Mo_2FeB_2 borides in the structure of specimen No. 1 (TiB_2 with d = 2–3 μm). However, in this case, the titanium content in the Mo_2FeB_2 compound attains 8 % that is somewhat higher than the Ti content in Mo_2FeB_2 structure of specimen No. 1 (Ti content is 6 %, and Mo content is 60 %). In the iron-based metallic matrix, the local formation of Fe–Fe_2B (Fig. 3d, Table 2, spectrums 4 and 5) and Fe–Mo_2FeB_2 eutectics (Fig. 3d, Table 2, spectrums 5 and 6) was detected. Due to the formation of the eutectic structure, the microhardness of the matrix reaches 5–6 GPa.

The microstructural investigations of specimen No. 3 (TiB_2 with d = 70–100 nm) revealed a heterophase matrix-type struc-

Table 2. Chemical composition of phases in the TiB_2–80 wt.%(Fe–13 wt.%Mo) composite material with TiB_2 particle size of 2–3 μm

Figure	Spectrum	Element composition, wt. %				Phase
		Ti	Fe	Mo	B	
3c	1	1	97	2	0	Fe-based solution
	2	64	2	—	34	TiB_2
	3	8	24	58	10	Mo_2FeB_2
3d	4	0	99	1	0	Fe-based solution
	5	1	89	1	9	Fe_2B
	6	6	25	59	10	Mo_2FeB_2

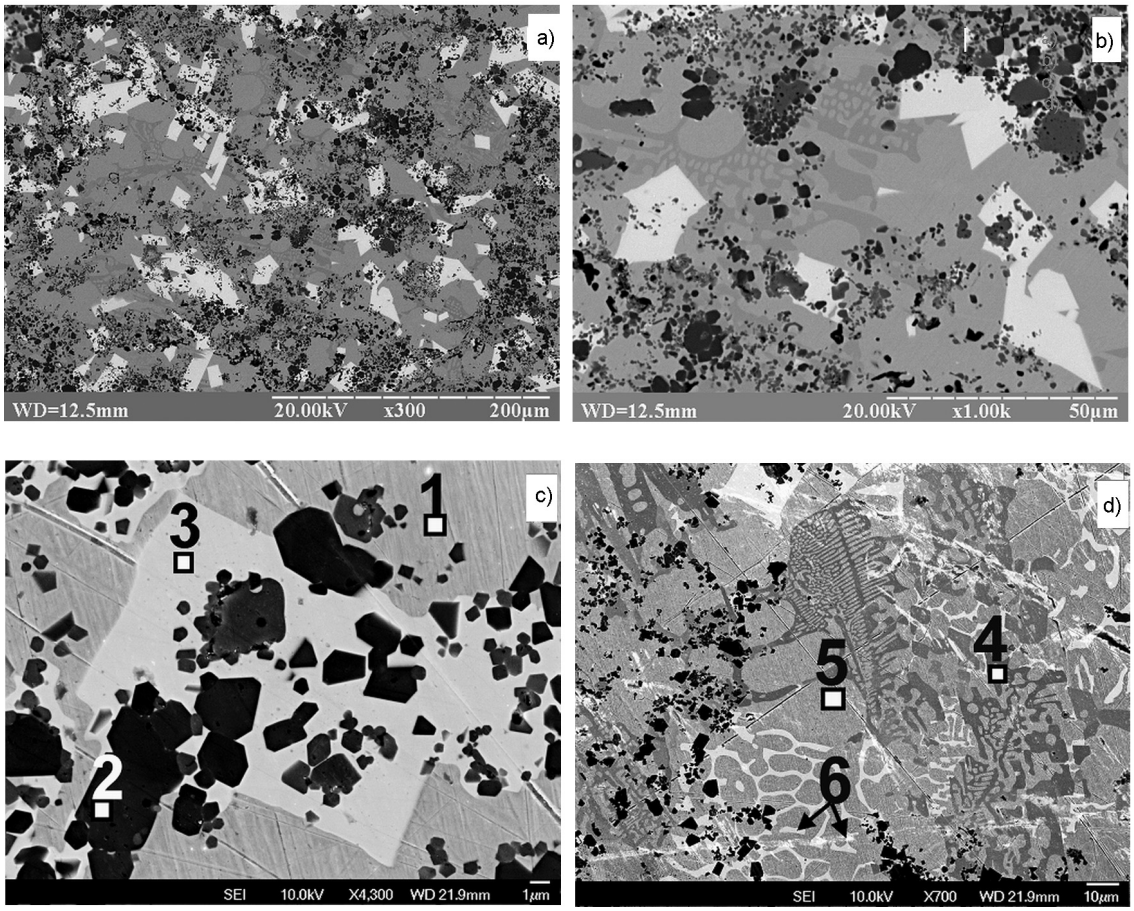

Fig. 3. Structure of the TiB_2–80 wt.%(Fe–13 wt.%Mo) composite material with the TiB_2 particle size of 2–3 μm: (a), (b) general view; (c) zone of Mo_2FeB_2 borides formation; (d) zone of eutectic formation.

ture (Fig. 4). The gray matrix is a solid solution of molybdenum (≤2 wt.%) and titanium (≤wt.1 %) in iron (Fig. 4c, Table 3, spectrum 1). In the structure of specimen No. 3, inclusions of a white phase identified as Mo_2FeB_2 boride were detected (Fig. 4c, Table 3, spectrum 2). In this case, at least 10 wt.% of Ti dissolve in the molybdenum-iron boride. The grain size of Mo_2FeB_2 borides in the structure of specimen No. 3 (TiB_2 with d = 70–100 nm) attains 100 μm, and the microhardness is 21–22 GPa. Moreover, dark gray inclusions with a size of 2–5 μm were detected in the structure of specimen No. 3. Microstructural investigations revealed the inhomogeneity of the composition of the dark grey phase: it contains about 19 wt.% B, 27 wt.% Ti, 41 wt.% Fe, and 13 wt.% Mo at the center (Fig. 4d, Table 3, spectrum 3) and about

Table 3. Chemical composition of phases in the TiB_2–80 wt.%(Fe–13 wt.% Mo) composite material with initial TiB_2 particle size of 70–100 nm

Figure	Spectrum	Element composition, wt.%				Phase
		Ti	Fe	Mo	B	
4	1	–	99	1	–	Fe-based solid solution
	2	10	25	55	10	Mo_2FeB_2
	3	27	41	13	19	complex boride
	4	46	6	19	29	TiB_2

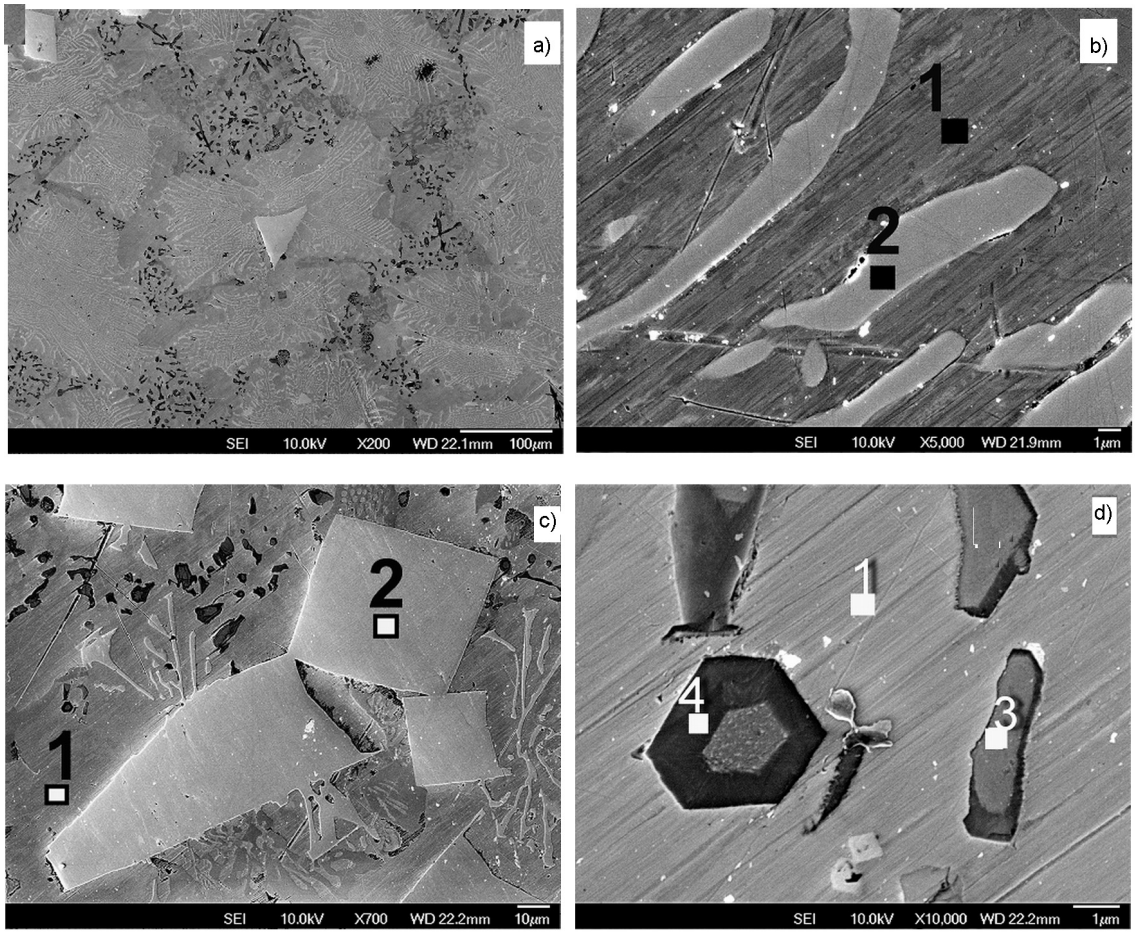

Fig. 4. Structure of the TiB_2–80 wt.%(Fe–13 wt.% Mo) composite material with the TiB_2 particle size of 70–100 nm: (a) general view; (b, c) zone of Mo_2FeB_2 borides formation; (d) zone of boride phases formation.

29 wt.% B, 46 wt.% Ti, 6 wt.% Fe, and 19 wt.% Mo on the periphery of the grains (Fig. 4d, Table 3, spectrum 4). It can be assumed that the dark gray phase is iron boride doped with titanium. The black phase is probably titanium diboride doped with molybdenum or with molybdenum and iron. As the content of the black phase (TiB_2) increases on the periphery, these inclusions acquire a regular hexagonal shape, which is typical for titanium diboride grains. It should be noted that the EPMA method did not detect titanium diboride particles with a size less than 1 μm in the structure of the composite material. A feature of the TiB_2(Fe–13 wt.% Mo) composite material No. 3 (TiB_2 with d = 70–100 nm) is the intensive formation of the Fe–Mo_2FeB_2 (Fig. 5, Table 4, spectra 1 and 2) and Fe–Fe2B eutectics (Fig. 5, Table 5, spectra 1 and 5).

Taking into account the results of DTA and microstructure investigations of TiB_2–

Table 4. Chemical composition of phases in the TiB_2–80 wt.%(Fe–13 wt.%Mo) composite materials with initial TiB_2 particle size of 70–100 nm

Spectrum	Element composition, wt.%				Phase
	Ti	Fe	Mo	B	
1	0	98	2	0	Fe-based solid solution
2	10	26	54	10	Mo_2FeB_2
3	28	42	12	18	complex boride
4	47	5	19	29	TiB_2
5	0	87	2	11	Fe_2B

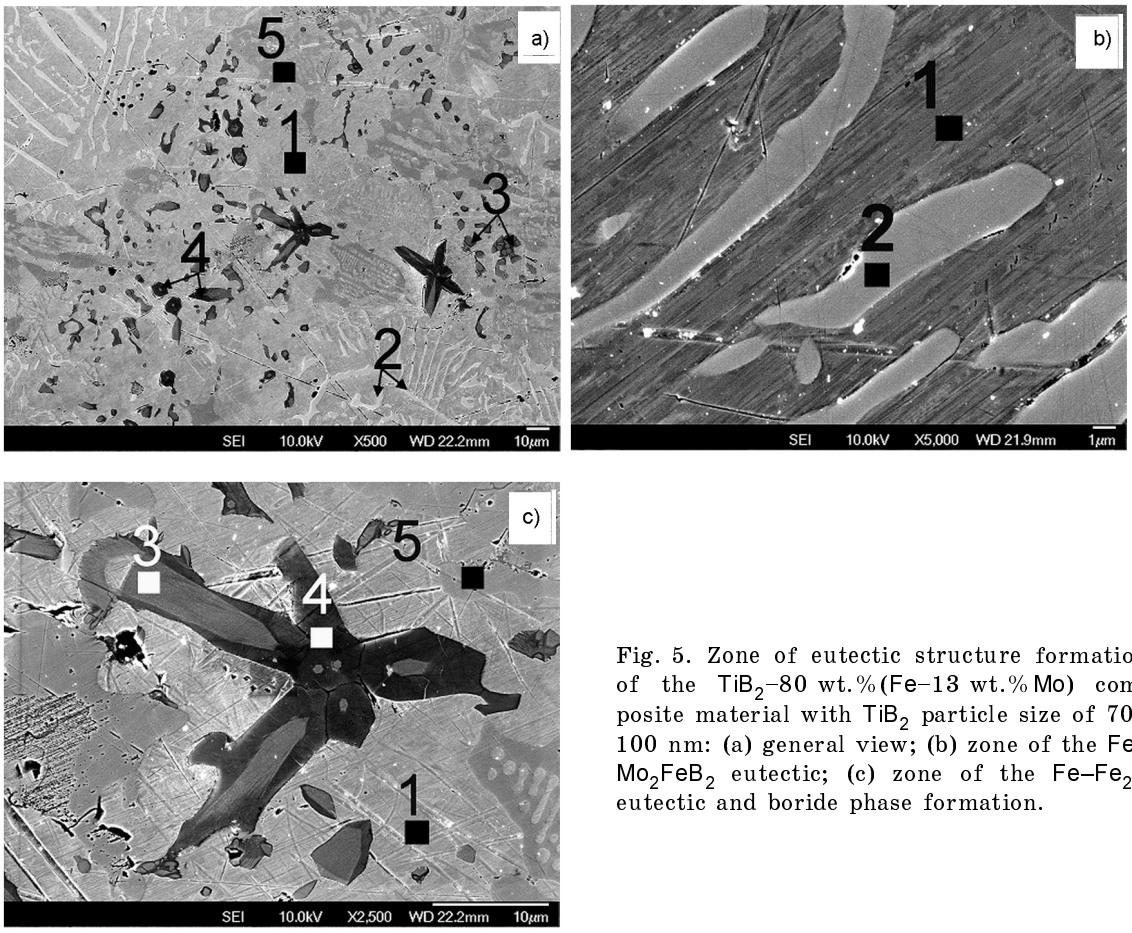

Fig. 5. Zone of eutectic structure formation of the TiB_2–80 wt.%(Fe–13 wt.%Mo) composite material with TiB_2 particle size of 70–100 nm: (a) general view; (b) zone of the Fe–Mo_2FeB_2 eutectic; (c) zone of the Fe–Fe_2B eutectic and boride phase formation.

80 wt.% (Fe–13 wt.% Mo) composite materials with different initial sizes of titanium diboride particles, the following conclusions can be made. Under conditions of liquid-phase sintering of specimens of the TiB_2–80 % (Fe–13 % Mo) composite materials with initial particle size of titanium diboride of 9–10 μm (specimen No. 1) and 2–3 μm (specimen No. 2), the partial dissolution of titanium diboride grains in the iron-based alloy occurs, and, in this case, the iron-based alloy is saturated by boron and titanium. Once the saturation limit of the solid solution by boron is attained, the formation of borides occurs. Since boron has a high affinity to molybdenum, Mo_2FeB_2 boride forms. This agrees with the data of [18], in which the formation of Mo_2FeB_2 grains of large sizes in the process of liquid-phase sintering at $T = 1320$°C was detected. In the present case, the exothermic effect in the temperature range of 1215–1550°C on the DTA heating curves of the composite materials corresponds to the dissolution process of TiB_2 and Mo_2FeB_2 borides. Titanium penetrates into the alloy from titanium diboride and partially dissolves in Mo_2FeB_2 borides.

Table 5. Size and chemical composition of Mo_2FeB_2 grains in the structure of the TiB_2–80 wt.%(Fe–13 wt.%Mo) composite materials with different TiB_2 particle sizes

	Initial particle size of TiB_2		
	9–10 μm	2–3 μm	70–100 nm
Grain size of Mo_2FeB_2 complex borides, μm	20–30	20–30	80–100
Ti content in grains of Mo_2FeB_2 complex borides, wt %	6	8	10

Under cooling of the composite material, the solubility of the elements (Mo, Ti, and B) in iron decreases, resulting in formation of the Fe–Fe_2B and Fe–Mo_2FeB_2 eutectics; this corresponds to two exothermic effects at 1160–1122°C and 1122–1060°C on the DTA cooling curves of these materials [19–21]. Due to the formation of Mo_2FeB_2 borides and the eutectics, the alloy is depleted in molybdenum, titanium, and boron, the total content of which in the iron-based matrix does not exceed 2 wt.%.

The effect of nanosized titanium diboride particles consists in the fact that a large interface area appears; this substantially affects the formation of the TiB_2–80 % (Fe–13 % Mo) composite material structure. Due to the nanosize factor, the intensive dissolution of titanium diboride particles in the iron-based alloy occurs and the Fe-based alloy becomes rapidly saturated by boron and titanium. According to the DTA data for specimen No. 3, the dissolution processes of titanium diboride grains begin already at a temperature of 1175°C, which is lower by 40°C than that for specimens No 1 (TiB_2 with d = 2–3 μm) and No. 2 (TiB_2 with d = 9–10 μm). Moreover, the exothermic effect on the DTA heating curves of specimen No. 3 is more pronounced than that of No. 1 and No. 2 specimens; this also confirms the intensification of the dissolution of TiB_2 particles. The intensification of these processes leads to the more intensive formation of inclusions of Mo_2FeB_2 complex borides. In particular, it should be noted that, with a decrease in the size of titanium diboride particles up to 70–100 nm, the size of Mo_2FeB_2 inclusions increases several times. In the structure of the TiB_2–(Fe–13 % Mo) composite materials with an initial particle size of titanium diboride of 9–10 μm and 2–3 μm, the size of Mo_2FeB_2 borides does not exceed 20–30 μm (Figs. 2 and 3, spectrum 3); whereas, in the structure of specimen No. 3 with additives of nanosized titanium diboride particles, their size attains 80–120 μm (Fig. 4, spectrum 2). It should be also noted that, at least 10 % Ti dissolve in Mo_2FeB_2 borides in the structure of specimen No. 3 (TiB_2 with d = 70–100 nm) (Fig. 4, spectrum 4); whereas, in the structure of specimens No 1 and No. 2 (TiB_2 with d = 9–10 and 2–3 μm, respectively), the titanium content in Mo_2FeB_2 borides does not exceed 6–8 % (Fig. 2, spectrum 3; Fig. 3, spectrum 3).

As noted above, in the structure of specimen No. 3 of the TiB_2–(Fe–13 % Mo) composite material, titanium diboride particles with a size less than 1 μm were not detected, and the formation of titanium diboride particles occurred on iron boride grains (Figs. 4 and 5). Taking into account the EPMA data, it can be assumed that, in the process of liquid-phase sintering of the TiB_2–(Fe–13 % Mo) composite material with an initial particle size of 70–100 nm, the complete dissolution of titanium diboride grains occurs with their subsequent recrystallization on grain boundaries of Fe_2B iron boride. Since identical exothermic effects are observed on the DTA heating curves of specimen No. 3 as well as for specimens No. 1 and No. 2, it can be assumed that the dissolution and recrystallization processes of TiB_2 occurs simultaneously during heating in the temperature range 1175–1550°C.

The formation of the eutectic structure in specimen No. 3 is also connected with the intensification of the dissolution of TiB_2 particles. In cooling, as a result of the decrease in the solubility of the elements in iron, the crystallization of a large amount of the Fe–Fe_2B and Fe–Mo_2FeB_2 eutectics occurs; this is represented by two exothermic effects at temperatures 1160–1122°C and 1122–1020°C on the DTA curves of specimen No. 3 as well as for specimens No. 1 and No. 2.

4. Conclusions

The formation of the structure of TiB_2–80 wt.% (Fe–13 wt.% Mo) composite materials is substantially influenced by the particle size of titanium diboride. It has been found that the interphase interaction processes in the TiB_2–80 wt.% (Fe–13 wt.% Mo) composite materials are intensified as the particle size of titanium diboride decreases.

The decrease in the particle size of titanium diboride down to 2–3 μm does not substantially affects the processes of formation of the structural-phase composition of the composite material. In the process of liquid-phase sintering of the TiB_2–80 wt.% (Fe–13 wt.% Mo) composite materials with an initial TiB_2 particle size of 2–3 μm and 9–10 μm, titanium diboride grains partially dissolve with subsequent formation of Mo_2FeB_2 borides, which are characterized by high hardness (20–22 GPa) and can increase the wear resistance of composite materials and coatings. The particle size of titanium diboride in the structure of the TiB_2–80 wt.% (Fe–13 wt.% Mo) composite materials does not significantly differ from their initial size; the grain size of Mo_2FeB_2 borides is 20–30 μm.

The addition of titanium diboride nanoparticles (70–100 nm) into the TiB_2–80 wt.% (Fe–13 wt.% Mo) composite material leads to an intensification of dissolution-recrystalization of titanium diboride; as a result, their size increases up to 5–6 μm. In this case, the eutectic structure with a large amount of Mo_2FeB_2 and Fe_2B borides forms, that leads to the material brittleness. The grain size of Mo_2FeB_2 borides increases up to 100 μm.

Thus, to obtain TiB_2–80 wt.%(Fe–13 wt.% Mo) composite materials by the liquid-phase sintering in vacuum, it is reasonable to use titanium diboride particles with a size of 2–10 μm; in this case, it is possible to produce a heterophase structure which combines hard grains of TiB_2 and Mo_2FeB_2 borides and a plastic metal matrix.

References

1. L.Prakash, Fundamentals and General Applications of Hardmetals, in: Comprehensive Hard Materials, Elsevier, Oxford (2014).
2. N.Wu, F.Xue, J.Wang et al., *Mater. Sci. Eng.*, **743**, 546 (2019).
3. S.Liu, D.Liu, *Int. J. Refract. Met. Hard Mater.*, **82**, 273 (2019).
4. T.P.Grebenok, T.V.Dubovik, M.S.Kovalchenko et al., *Powder Metall. Metal Ceram.*, **55**, 48 (2016).
5. J.M.Sanchez, I.Azcona, F.Castro, *J. Mater. Sci.*, **35**, 9 (2000).
6. V.P.Konoval, V.Zh.Shemet, B.Grushko et al., *Powder Metall. Metal Ceram.*, **51**, 429 (2012).
7. M.S.Storozhenko, A.P.Umanskii, A.V.Lavrenko et al., *Powder Metall. Metal Ceram.*, **50**, 719 (2012).
8. A.P.Umanskii, A.E.Terentiev, M.Storozhenko, I.S.Marsenyuk, *Powder Metall. Metal Ceram.*, **53**, 359 (2015).
9. X.Wang, H.Shun, C.Li et al., *Surf. Coat. Technol.*, **201**, 2500 (2006).
10. C.M.Chun, N.V.Bangaru, N.Thirumalai et al., *Int. J. Appl. Ceram. Technol.*, **5**, 597 (2008).
11. I.M.Spiridonova, A.D.Panasyuk, E.V.Sukhovaya, A.P.Umanskii, Stabilnost Kompozitsionnykh Materialov, Svindler A.L., Dnepropetrovsk (2011).
12. P.S.Kislyi (editor), Kermety, Naukova Dumka, Kiev (1985).
13. A.Panasyuk, O.Umanskyi, M.Storozhenko, V.Akopyan, *Key Eng. Mater.*, **527**, 9 (2013).
14. M.S.Storozhenko, *Powder Metall. Metal Ceram.*, **56**, 617 (2017).
15. M.S.Storozhenko, O.P.Umanskyi, O.U.Stelmach et al., *Powder Metall. Metal Ceram.*, **57**, 200 (2018).
16. M.S.Storozhenko, A.P.Umanskii, A.E.Terentiev, I.M.Zakiev, *Powder Metall. Metal Ceram.*, **56**, 60 (2017).
17. N.Wu, F.Xue, H.Yang et al., *J. Ruan. Ceram. Int.*, **45**, 1370 (2019).
18. H.Yu, W.Liu, Y.Zheng, *Mater. Des.*, **32**, 3521 (2011).
19. E.I.Gladyshevskii, T.F.Fedorov, Y.B.Kuz'ma, R.V.Skolozdra, *Sov. Powder Metall. Met. Ceram.*, **5**, 305 (1966).
20. A.Antoni-Zdziobek, M.Gospodinova, F.Bonnet, F.Hodaj, *J. Phase Equilib. Diff.*, **35**, 701 (2014).
21. A.Antoni-Zdziobek, M.Gospodinova, F.Bonnet, F.Hodaj, *J. Alloys Compd.*, **657**, 302 (2016).